

Relativistic Effects in Proper Motions of Stars Surrounding the Galactic Center

M. Jaroszyński

Warsaw University Observatory, Al. Ujazdowskie 4, 00-478 Warszawa,
Poland
e-mail: mj@sirius.astrouw.edu.pl

Received November 16, 1998

ABSTRACT

We simulate the astrometric observations of stars moving close to the black hole in the Galactic Center. We show, that for orbits $\leq 10^3$ AU and position measurements with the accuracy of the Keck Interferometer, the periastron motion of elliptical orbits will be measurable. The models of star trajectories neglecting the periastron motion will be easy to reject with the high confidence level. The measurement of orbital elements and the periastron motion can be effectively used as an independent estimate the distance to the Galactic Center. The effects of orbit precession may be visible in some cases. The effects of gravitational radiation are completely negligible as well as the influence of the black hole rotation on the propagation of light.

galaxies:black holes - galaxies: individual (Milky Way) - gravitational lensing - relativity

1 Introduction

The proper motion studies of stars in the Galactic Center (Eckart et al. 1995, Genzel et al. 1996, 1997, Ghez et al. 1998) have shown the astonishing accuracy of astrometric observations in the near infrared K band. Their studies have proved the existence of a very compact dark mass, most likely a black hole of $\sim 2.6 \times 10^6 M_{\odot}$. The closest investigated star is at the projected distance 100 mas, which corresponds to ~ 850 AU. The gravitational radius for the quoted mass, $GM/c^2 = 0.025$ AU and corresponds to $3 \mu\text{s}$. Thus the motion at $\sim 3 \times 10^4$ gravitational radii from the mass is already observed.

Jaroszyński & Paczyński (1998, hereafter JP98) have investigated the possibility of finding orbital parameters for stars near the Galactic Center.

According to their work the systematic observations of the closest star included in the proper motion studies can be sufficient to define its orbit in ~ 10 y with the accuracy allowing for the determination of the central mass with an error smaller than the present estimates. Increased accuracy of astrometric measurements and ability to observe fainter stars which may be found closer to the center, will allow for still more accurate determinations in shorter time.

The speckle interferometry with the Keck telescope (Ghez et al. 1998) reaches the resolution ~ 50 mas and the accuracy of ~ 2 mas in position measurements. The Keck Interferometer, which is now under construction (van Belle & Vasisht 1998) will have ~ 5 mas resolution and $\sim 20 \mu\text{as}$ (0.17 AU) astrometric accuracy. It will be able to measure the position of a faint point object with $K \leq 22^m$ if a bright $K \leq 14^m$ star can be found within a circle of the radius ≤ 20 arcsec around it. Such measurement accuracy, up to few gravitational radii, suggests the possibility of investigating relativistic corrections to the motion of stars sufficiently close to the central mass. We include the periastron motion, the precession of the orbit, the gravitational radiation from the star-central mass binary, and the bending of rays in our study.

In this paper we assume that there is a $\sim 2.6 \times 10^6 M_\odot$ black hole in the Galactic Center and we investigate the measureability of the relativistic effects in its vicinity. We consider orbits of stars of sizes 50 to 1000 AU, which correspond to periods 0.219 to 19.6 y. Following JP98 we use Monte Carlo method to simulate the observations of the stars. We use minimization algorithms to fit the model trajectories to the synthetic data sets. Using models with different level of sophistication and comparing the results we are able to find which relativistic effects must be included in the interpretation of observations and which are below the current and near future detection limits.

In the next Section we describe the motion of particles and photons in the weak gravitational field of a rotating body. In Section 3 we present the methods of simulating the observations and procedures of parameter fitting. We also present the main results of this paper - the range of orbit sizes for which the study of relativistic effects is possible with given astrometric accuracy. We also calculate the accuracy of the distance estimate based on the measured periastron motion. In Section 4 we estimate the chance that a star (stars) bright enough to be followed by the Keck Interferometer may be found close enough to the Galactic Center, so the relativistic effects are measurable. The conclusions follow in the last Section.

2 Equations of motion in the weak field approximation

We describe the gravitational field far from a rotating black hole in the isotropic coordinates t , x , y , and z . We use the geometrical units for mass (M) and angular momentum (J) of the hole:

$$m \equiv \frac{GM}{c^2} \quad j \equiv \frac{J}{Mc} \quad (1)$$

where G is the gravity constant and c is the velocity of light. The black hole angular momentum is directed along $\mathbf{e}_z \equiv \mathbf{k}$. The observer is in the $(\mathbf{e}_x, \mathbf{e}_z)$ plane. In the approximation preserving terms of the order $\sim r^{-2}$, the lowest including effects of the black hole angular momentum, the metric takes the form (Landau & Lifshitz 1973):

$$ds^2 = - \left(1 - 2\frac{m}{r} + 2\frac{m^2}{r^2} \right) dt^2 + 4\frac{jmy}{r^3} dt dx - 4\frac{jmx}{r^3} dt dy + \left(1 + 2\frac{m}{r} + \frac{3m^2}{2r^2} \right) (dx^2 + dy^2 + dz^2) \quad (2)$$

2.1 Orbits of Stars

In the weak field approximation the orbit of the star can be described as a classical ellipse of semimajor axis a and eccentricity e in a non-inertial frame of reference with coordinates (x_1, y_1, z_1) . We assume that the black hole is at the origin of this coordinate system, the orbit is at the $(\mathbf{e}_{x_1}, \mathbf{e}_{y_1})$ plane, and \mathbf{e}_{x_1} points toward the orbit periastron. The orientation of the frame is such that the orbital angular momentum is directed along the positive direction of $\mathbf{e}_{z_1} \equiv \mathbf{n}$. The inclination i of the orbital plane relative to the equatorial plane is given by the condition $\cos i = (\mathbf{k}\mathbf{n})$. The ascending node of the orbit is at the position angle Ω measured from the x axis. The periastron is at the angle ω from the ascending node. Finally the position of the star on the orbit, as measured by the eccentric anomaly u , is given by the Kepler equation:

$$\frac{2\pi}{P}(t - t_0) = u - e \sin u \quad x_1 = a(\cos u - e) \quad y_1 = a\sqrt{1 - e^2} \sin u \quad (3)$$

where P is the orbital period and t_0 is the time of the passage through the periastron.

The Lense-Thirring effect causes the precession of the orbital plane and the change of the periastron location. As a result the line of nodes rotates with the angular velocity:

$$\dot{\Omega}_{\text{prec}} = \frac{2jmc}{a^3(1-e^2)^{3/2}} \quad \dot{\Omega} = \dot{\Omega}_{\text{prec}} \sin i \quad (4)$$

and the periastron position changes with the rate:

$$\dot{\omega}_{\text{prec}} = -3\dot{\Omega}_{\text{prec}} \cos i \quad (5)$$

Independently of the black hole angular momentum, the periastron of the orbit advances with the angular velocity:

$$\dot{\omega}_{\text{per}} = \frac{3m^{3/2}c}{a^{5/2}(1-e^2)} \quad (6)$$

The resulting evolution of the orbit orientation is given as:

$$\Omega = \Omega_0 + \dot{\Omega}(t - t_0) \quad \omega = \omega_0 + (\dot{\omega}_{\text{per}} - 3\dot{\Omega}_{\text{prec}} \cos i)(t - t_0) \quad (7)$$

where Ω_0 and ω_0 are the initial values of the angles. The star location at any reference frame can be calculated after a straightforward coordinate transformation based on the equation:

$$\mathbf{r}(t) = x_1(t) \mathbf{e}_{\mathbf{x}_1}(t) + y_1(t) \mathbf{e}_{\mathbf{y}_1}(t) \quad (8)$$

Suppose an observer is located in the (x, z) plane at the angle Θ measured from the hole rotation axis. The observed position of the star on the sky is given as:

$$Y(t_{\text{obs}}) = y(t) \quad Z(t_{\text{obs}}) = z(t) \sin \Theta - x(t) \cos \Theta \quad (9)$$

where we have chosen coordinates in the sky with Z axis along the projection of the black hole angular momentum and Y axis along the y axis of our frame. The position angle ψ , which gives the orientation of the Z axis on the sky is another parameter of the problem. The time of the observation t_{obs} depends on the source position and is given (up to an additive constant) as:

$$ct_{\text{obs}} = ct - x(t) \sin \Theta - z(t) \cos \Theta \quad (10)$$

2.2 The Influence of Gravitational Lensing

In the typical lensing situation the source and the observer are far from the lens, but the rays pass through its close vicinity. Such case of lensing near the Galactic Center has been considered by Wardle & Yusef-Zadeh (1992), Jaroszyński (1998), and Alexander & Sternberg (1998). In such a case one can describe a ray as two segments of a straight line deflected in the lens plane. In our case the distance of the source from the lens is of the same order as the encounter parameter for rays and the standard gravitational lensing formalism can not be employed. Instead we consider the null geodesics in the metric of Eq. 2.

In the zeroth order approximation a ray is a straight line. We assume that the point of the closest approach to the hole is at \mathbf{b}_0 . Suppose the ray is propagating along the unit vector \mathbf{l} and let l be the length measured along the ray from the point of the closest approach. Since we are using the weak field approximation, we have to limit ourselves to the case $b_0 \gg m$. For a unit energy photon propagating along the ray the components of the four momentum are: $p_t = -1$, $p^t = 1$, $p_l = 1$, $p^l = 1$, and all other vanish.

In the first order approximation we include the terms proportional to m/r in the metric, which preserves its spherical symmetry. Due to this symmetry the ray remains in the plane $(\mathbf{b}_0, \mathbf{l})$ and is deflected toward the hole:

$$\frac{d}{dl}p_b = \frac{1}{2}g_{tt,b}p^t p^t + \frac{1}{2}g_{ll,b}p^l p^l = -\frac{2mb_0}{r^3} \quad (11)$$

where $r = \sqrt{b_0^2 + l^2}$. Integrating the above equation with the boundary condition at the observer position: $p_b = 0$ for $l = \infty$, one gets

$$p_b(l) = \frac{2m}{b_0} \left(1 - \frac{l}{\sqrt{b_0^2 + l^2}} \right) \quad (12)$$

For sources far behind the lens the photon momentum changes its direction by an angle $(p_b(+\infty) - p_b(-\infty))/p_l = -4m/b_0$, which is a standard result for a ray deflection. The photon momentum perpendicular to the ray is a first order quantity, so $p^b = p_b$. Integrating again and assuming $b(+\infty) = b$ we have:

$$\frac{d}{dl}b(l) = p^b \quad b(l) = b - \frac{2m}{b_0} \left(\sqrt{b_0^2 + l^2} - l \right) \quad (13)$$

where the second relation is the analog of the lens equation. For $l = 0$ one has $b_0 = b - 2m$ which is the relation between the observed source

position (b) and the encounter parameter (b_0). In general the source is at the distance b_s from the optical axis, at the position l_s along the ray. The value of the encounter parameter b_0 can be obtained as a solution to the equation $b(l_s) = b_s$. In a typical case, when $b_s \gg m$, the same is true of b and b_0 and one has approximately:

$$b = b_s + \frac{2m}{b_s} \left(\sqrt{b_s^2 + l^2} - l \right) \quad (14)$$

The formula is valid for $|l| \leq b_s^2/m$. In the language of gravitational lensing it means, that the source should be at a distance much larger than Einstein radius from the optical axis.

The second order terms ($\sim m^2/r^2$) in the diagonal metric components introduce only quantitative corrections to the lens equation. The off diagonal terms introduce the dependence of geodesics on the black hole angular momentum. The deflection of rays is not necessarily toward the hole. Since the metric components of interest are of the second order, the influence of the hole angular momentum can be calculated along the zeroth order rays. Only the deflection perpendicular to the line of sight is interesting. In the observer's coordinates the geodesic equations are:

$$\frac{d}{dl} p_Y = \frac{2jm \sin \Theta}{r^3} - \frac{6jmY_0^2 \sin \Theta}{r^5} \quad (15)$$

$$\frac{d}{dl} p_Z = -\frac{6jmY_0Z_0 \sin \Theta}{r^5} \quad (16)$$

where the encounter vector is given as $\mathbf{b}_0 = (Y_0, Z_0)$ and the distance from the hole as $r = \sqrt{b_0^2 + l^2}$. The integration gives:

$$\delta Y = \frac{2jm \sin \Theta}{b_0^4} (Z_0^2 - Y_0^2) \left(\sqrt{b_0^2 + l^2} - l \right) + \frac{2jm \sin \Theta Y_0^2}{b_0^2 \sqrt{b_0^2 + l^2}} \quad (17)$$

$$\delta Z = -\frac{4jmY_0Z_0 \sin \Theta}{b_0^4} \left(\sqrt{b_0^2 + l^2} - l \right) + \frac{2jmY_0Z_0 \sin \Theta}{b_0^2 \sqrt{b_0^2 + l^2}} \quad (18)$$

where δY , δZ denote the angular momentum induced shift of the ray from a trajectory neglecting these effects. Even for the maximally rotating black hole ($j = m$), the shifts are of the order $\sim m m/b_0 \ll m$ and we neglect them in further calculations.

2.3 The Gravitational Radiation

The gravitational radiation lowers the energy of a binary system of masses leading to the orbit narrowing and shortening of the orbital period. For two masses M_1 and M_2 at a distance r from each other, moving on circular orbits, one has (Landau & Lifshitz 1973):

$$\dot{r} = -\frac{64G^3M_1M_2(M_1 + M_2)}{5c^5r^3} \quad (19)$$

We estimate the relative change of the orbit size for a star with mass $M_2 = 2.6M_\odot$ revolving around a black hole of the mass $M_1 = 2.6 \times 10^6 M_\odot$. We get

$$\frac{|\dot{r}P|}{r} \approx 10^{-13} \left(\frac{100\text{AU}}{r} \right)^{2.5} \quad (20)$$

which means that the gravitational radiation can be neglected for a wide range of star masses and orbit sizes.

3 Observability of the Relativistic Effects

We simulate the astrometric observations of stars on elliptic orbits around the Galaxy Center black hole. We check for which range of orbital periods the measurement of the star proper motion with given positional accuracy is sufficient to measure the rate of the periastron motion. We also check, whether the precession of the orbital plane, which may be present if the black hole is rotating, can cause any measurable effects.

The simulations consist of two parts. First we choose the physical parameters of the orbits (a , e , P), their orientation in space (i , Ω_0 , ω_0) and time (t_0). The value of the semimajor axis is the main parameter of this study and it covers a range of values. We use the linear measure of the orbit semimajor axis a , while the quantity more directly related to observations is the corresponding angle α ($a \equiv \alpha R$, where R is the distance to the Galactic Centre, for which we use $R = 8.5$ kpc). The orbital period is related to the orbit size, since we assume that the black hole has the mass $M = 2.6 \times 10^6 M_\odot$ (Ghez et al. 1998). Other parameters are chosen at random for each orbit. We assume that any orientation of the orbit in space and any initial phase of the orbital motion have equal probabilities. The initial time of the measurement seems to be unimportant, but due to the fact that the conditions for astronomical ground observations of Sgr A* do

change through the year, we treat t_0 as another random variable. For simplicity we assume, that the observations are possible from March through September or from the 10-th to the 40-th week of the year. We do not introduce any seasonal or random dependence of the accuracy of the astrometric measurements on time. The rate of the periastron motion $\dot{\omega}$ and the precession angular velocity $\dot{\Omega}$ can be calculated, when other orbital parameters are known.

The equations of Sec. 2 can be used to obtain the “true” trajectory of the star projected into the plane of the sky $\mathbf{X}(t; t_0, a, e, p, i, \Omega_0, \omega_0, \dot{\Omega}, \dot{\omega}, \Theta, \psi)$, or $\mathbf{X}(t)$ in short notation. Observations of the star in the instants of time $\{t_j\}$ give the measured values of its positions in the sky $\{\mathbf{X}_j\}$. We simulate the process of observation assuming that

$$\mathbf{X}_j = \mathbf{X}(t_j) + \delta\mathbf{X}_j \quad (21)$$

where $\delta\mathbf{X}_j$ are the errors introduced by observations. We assume that each component of the position vector is measured with errors which are normally distributed with dispersion σ and vanishing mean value. Equivalently the distribution of $\delta\mathbf{X}_j$ is given as:

$$P\{|\delta\mathbf{X}_j| > s\} = \exp\left(-\frac{s^2}{2\sigma^2}\right) \quad (22)$$

and the direction of $\delta\mathbf{X}_j$ has a uniform distribution. Using Monte Carlo method we obtain synthetic data sets $\{\mathbf{X}_j\}$ representing the sequences of astrometric observations with noise.

The next step is to fit a model to each synthetic data set. We fit orbital parameters to the observations by minimizing the expression:

$$\chi^2 = \sum_{j=1}^N \frac{(\mathbf{X}_j - \mathbf{X}(t_j; t_0, a, e, P, i, \Omega_0, \omega_0, \dot{\Omega}, \dot{\omega}, \Theta, \psi))^2}{\sigma^2} \quad (23)$$

The parameters fitted to a synthetic data set are different from the original “true” parameters of the orbit. Many simulations of synthetic data sets for the same orbit give the scatter in estimated parameters. This “bootstrap” method (Press et al. 1988) is a practical way to estimate the accuracy of parameter fitting in the case of real observations.

The synthetic data sets we obtain using Monte Carlo method are always based on calculations including the effects of the periastron motion, the precession of the orbit and the bending of rays by gravitational lensing. To

check whether these effects are observable we compare the quality of the fits obtained with models including or neglecting them. We start from the simplest model which neglects both the precession and periastron motion of the orbit. Since we are limiting ourselves to the first order effects in gravitational lensing, the angular momentum of the black hole has no influence on the visual orbit and the reference frame defined by the hole rotation axis loses its observational basis. The inclination of the orbit should now be defined relative to the plane of the sky. The position of the line of nodes can be measured from the declination circle. We obtain the fits by minimizing χ^2 again, but using a simplified model $\hat{\mathbf{X}}(t; t_0, a, e, P, i, \Omega_0, \omega_0)$ instead of the full model depending on the higher number of parameters. This can also be achieved by fixing the values of some parameters ($\dot{\Omega} \equiv 0$, $\dot{\omega} \equiv 0$, $\Theta \equiv 0$, and $\psi \equiv 0$) in the full model. As we show in Fig. 1 the model neglecting the periastron motion and the precession of the orbit can be rejected for sufficient accuracy of position measurements and short orbits.

The precession of the orbit is a weaker effect than the periastron motion. If the observations span only a few orbital periods, which is the case of our simulations, the two effects can be difficult to distinguish. To clarify this point we try a model which includes periastron motion but neglects the precession, $\hat{\mathbf{X}}(t; t_0, a, e, P, i, \Omega_0, \omega_0, \dot{\omega})$. Our calculations show, that in this case the successful fits are possible. By successful we mean the fits with sufficiently low value of χ^2 :

$$\chi^2 \leq \chi_{0.95}^2(m) \quad (24)$$

where $m = 2N - 8$ is the number of the degrees of freedom for N observed positions and 8 parameters fitted. The subscript denotes the confidence level. (See also the dotted line on Fig. 1.)

Using the fitted orbital parameters one can calculate the mass of the central body with the help of the Third Kepler Law:

$$m = \frac{4\pi^2 a^3}{c^2 P^2} \quad (25)$$

Assuming that the central body is not rotating, one has the expected periastron motion per one revolution:

$$\Delta\omega_{\text{exp}} = \dot{\omega}_{\text{per}} P = \frac{6\pi m}{a(1 - e^2)} \quad (26)$$

We introduce another variables, independent of orbit eccentricity, which also measure the periastron motion:

$$Q_{\text{exp}} = \Delta\omega_{\text{exp}}(1 - e^2) \quad Q_{\text{fit}} = \dot{\omega}_{\text{fit}} P_{\text{fit}}(1 - e^2) \quad (27)$$

The first variable is based on the theory and fitted values of mass and semimajor axis of the orbit. The second is based on the fitted values of the periastron motion and the orbital period. For the nonrotating central body the variables should be equal. If the central body rotates, they should be different. Since both variables are based on the fitting procedure and "observations" with errors we can only compare their averaged values. We define:

$$D = \frac{\langle |Q_{\text{fit}} - Q_{\text{exp}}| \rangle}{\langle Q_{\text{exp}} \rangle} \quad (28)$$

$$S = \frac{\sqrt{\langle (Q_{\text{exp}} - \langle Q_{\text{exp}} \rangle)^2 \rangle}}{\langle Q_{\text{exp}} \rangle} \quad (29)$$

where the averages are taken for orbits of the same "true" semimajor axis a_0 and the same accuracy of astrometric observations σ . In Fig. 2 we compare the fitted and expected rates of periastron motion. We consider the case of stars moving in the gravitational field of a nonrotating black hole (left panel) and the case of maximally rotating hole (right panel). The left panel shows that the difference between the fitted and expected values scales linearly with the error in astrometric measurements. The same is true of the dispersion in the expected rate of periastron motion. This shows, that the differences are statistical in nature. The plots also show that the "observations" which cover a given number of rotational periods (5-10 in most cases) allow for a more accurate fit to the orbit semimajor axis and period than for a fit to the rate of the periastron motion. The right panel shows a nonlinear behavior. Comparing Eqs. 4, 5, and 6 one can get a rough estimate:

$$\frac{\Delta\omega_{\text{prec}}}{\Delta\omega_{\text{per}}} \sim \sqrt{\frac{j^2}{ma}} = \sqrt{\frac{m}{a}} \quad (30)$$

where we have assumed $|\cos i| = 0.5$ and neglected the factor dependent on the eccentricity. The second equality is valid for the maximally rotating hole ($j = m$). The presence of the precession in the "true" motion, which is not accounted for in the model causes a systematic difference between the rates of the periastron motion estimated in two ways. This difference remains finite when the error in measurements becomes very small. Its value is in agreement with the above formula for the orbits we consider. (Orbits with $a = 50, 150,$ and 250 AU or $P = 0.22, 1.14,$ and 2.45 y are considered here.)

The expected contribution to the periastron motion from the precession is smaller than $\sim 1\%$ for sufficiently wide orbits ($a \geq 250$ AU), even for the

maximally rotating central black hole. If we neglect this effect, Eqs. 25, 26 can be used as two independent methods of estimating the mass. After substitution we get the relation between the fitted variables of our model:

$$\Delta\omega = \frac{24\pi^3}{c^2} \frac{a^2}{(1-e^2)P^2} \quad (31)$$

In our approach we generate the synthetic data sets using a fixed distance to the Galactic Center, which makes the linear (a) and angular (α) measures of the semimajor axis indistinguishable. In reality the angular size of the orbit α is fitted directly, while its physical dimension can be calculated for the known distance to the object. Substituting $a = \alpha R$ to the above equation we get:

$$R = \sqrt{\frac{(1-e^2)\Delta\omega}{24\pi^3} \frac{cP}{\alpha}} \quad (32)$$

where all the variables in the RHS can be obtained from a fit to the observations. Thus we have a method of estimating the distance to the Galactic Center independent of any “standard candles”.

We have estimated the error in the distance found by the above method for a limited number of simulations. We have assumed that the black hole is maximally rotating, so the errors resulting from the precession (which is unaccounted for in the fitting procedure) are contained in our analysis. The most important contribution to the error comes from the measurement of the periastron motion despite the square root dependence of the distance on this variable. The distances calculated for orbits of given size are scattered. We find the median value of fitted distances R_{med} and such ΔR , that 68% of the results belongs to $[R_{\text{med}} - \Delta R, R_{\text{med}} + \Delta R]$. The plots of the relative error in the distance measurement are given in Fig. 3. Only the position measurements with errors smaller than $\sim 100 \mu\text{as}$ can give the distance estimate with the accuracy better than $\sim 10\%$.

4 Stars Very Close to the Galactic Center

The presence of stars at distances of few hundreds astronomical units from the Galactic Center is necessary to measure the effects we consider. A more detailed consideration of this subject can be found in JP98. The observations of Eckart & Genzel (1997), Genzel et al. (1996, 1997) and Ghez et al. (1998) show the presence of the dense central star cluster. The subset of stars with measured proper motions, which is seen close to the center in projection, is

also close to it in 3D, since the proper velocities of stars are related to the projected distance - a fact hard to understand for background or foreground objects. These stars are relatively bright ($K \leq 17^m$), but their sample is not complete (Ghez et al. 1998). This makes the following reasoning a bit risky. Assuming that the stars with measured proper motions are otherwise typical we can postulate that their luminosity function is the same as that of the central star cluster. The integral luminosity function for the Galactic Center in K can be obtained from papers of Blum et al. (1996) and Holtzman et al. (1998). It has a shape $N(\geq L_K) \sim L_K^{-\beta}$, with $\beta = 0.875$, and flattens at $K \approx 21^m$. Thus going from $K = 17^m$ to $K = 21^M$ makes the star volume density ~ 25 times higher and the typical distances between the stars in 3D become ~ 3 times smaller. Since the closest to the center observed star is at the distance ~ 850 AU, one can expect few fainter stars to be even closer. Thus the presence of observable stars at required distance from the center is likely.

5 Conclusions

We have investigated the observability of relativistic effects in motion of stars in the vicinity of the Galactic Center assuming the presence of massive black hole there and the accuracy of astrometric position measurements up to $\sim 20 \mu\text{as}$. We have shown that the gravitational radiation from the star-black hole binary and the second order effects in the deflection of rays related to the angular momentum of the black hole are completely negligible. The only robust effect is the motion of the orbit periastron. Systematic observations of a star orbit, covering ~ 25 y or ~ 5 orbital periods (whichever takes shorter) are sufficient to measure the rate of the periastron motion. With the accuracy of position measurements ~ 0.1 mas or better, it is possible to reject models neglecting the periastron motion for orbits of semimajor axis up to ~ 500 AU. With the highest accuracy expected for the Keck Interferometer ($\sim 20 \mu\text{as}$) it will be possible to measure the periastron motion for orbits up to $a \sim 10^3$ AU.

If the black hole in the Galactic Center is rotating it should cause the precession of the orbits of stars. We investigate this effect for orbits of the size $a = 50$ AU to 1000 AU. The effect is weak. The models of orbits neglecting the precession can not be rejected on the basis of the χ^2 value. This is probably due to the fact that precession of the orbit, when observed through a small number of revolution periods is hard to distinguish from

the periastron motion. (Both effects change the direction of the ellipse axes in space. Precession can also change the visual shape of the orbit, since it changes the angle between the line of sight and the orbital plane, but this is a very slow process.) The effects of precession can be seen indirectly as a discrepancy between the theoretical rate of periastron motion for a nonrotating black hole of estimated mass and the rate actually measured.

The measurements of the orbit elements (size, eccentricity, and period) and of the rate of the periastron motion can be used to estimate the distance to the source. This method is independent of any standard candles. The systematic observations of a star moving at distances $\leq 10^3$ AU from the Galactic Center with the maximal positional accuracy of the Keck Interferometer would give its distance up to few percent.

Acknowledgements. I thank Bohdan Paczyński for many useful discussions and the anonymous referee for his suggestions. This work was supported in part by the Polish State Committee for Scientific Research grant 2-P03D-012-12.

REFERENCES

- Alexander, T. & Sternberg, A. 1998, , , astro-ph/9811038.
 Blum, R.D., Sellgren, K., & DePoy, D.L. 1996, *ApJ*, **470**, 864.
 Eckart, A., & Genzel, R. 1997, *MNRAS*, **284**, 576.
 Eckart, A., Genzel, R., Hofmann, B., Sams, B.J., & Tacconi-Garman, L.E. 1995, *ApJ*, **445**, L23.
 Genzel, R., Eckart, A., Ott, T., & Eisenhauer, F. 1997, *MNRAS*, **291**, 219.
 Genzel, R., Thatte, N., Krabbe, A., Kroker H. & Tacconi-Garman, L.E. 1996, *ApJ*, **472**, 153.
 Ghez, A.M., Klein, B.L., Morris, M., & Becklin, E.E. 1998, *ApJ*, , in press, astro-ph/9807210.
 Holtzman, J.A., Watson, A.M., Baum, W.A., Grillmair, C.J., Groth, E.J., Light, R.M., Lynds, R. & O'Neil, E.J. 1998, *AJ*, **115**, 1946.
 Jaroszyński, M. 1998, *Acta Astron.*, **48**, 413.
 Jaroszyński, M. & Paczyński, B. 1998, , , *in preparation*.
 Landau, L.D. & Lifshitz, E.M. 1973, *Teoria Polia*, , Nauka (Moscow) .
 Press, W.H., Teukolsky, S.A., Vettering, W.T., & Flannery, B.P. 1988, *Numerical Recipes: the Art of Scientific Computing* (Cambridge University Press, Cambridge), , .
 van Belle, G.T. & Vasisht, G. 1998, *The Keck Interferometer: Science Requirements Document*, *JPL D-15477*, , <http://huey.jpl.nasa.gov/keck/>).
 Wardle, M. & Yusef-Zadeh, F. 1992, *ApJ*, **387**, L65.

7 Note Added in Proof

The highest astrometric accuracy of the Keck Interferometer ($\sim 20 \mu\text{as}$) will in fact be limited to relatively bright objects with $K \leq 17.6$. Thus the measurement of the periastron motion will probably be possible only for stars already discovered. The best candidate seems to be the star S0-1 from the Ghez et al. (1998) catalog. For the fainter stars the accuracy of position measurements will be much worse, $\sim 3 \text{ mas}$, not adequate for the following of the periastron motion. The results of our calculations can still be applied to observations done with other instruments providing high astrometric accuracy for faint objects, which may become operational in the future. I am grateful to Dr. Gerard T. van Belle for pointing to me my wrong interpretation of the Keck Interferometer technical data.

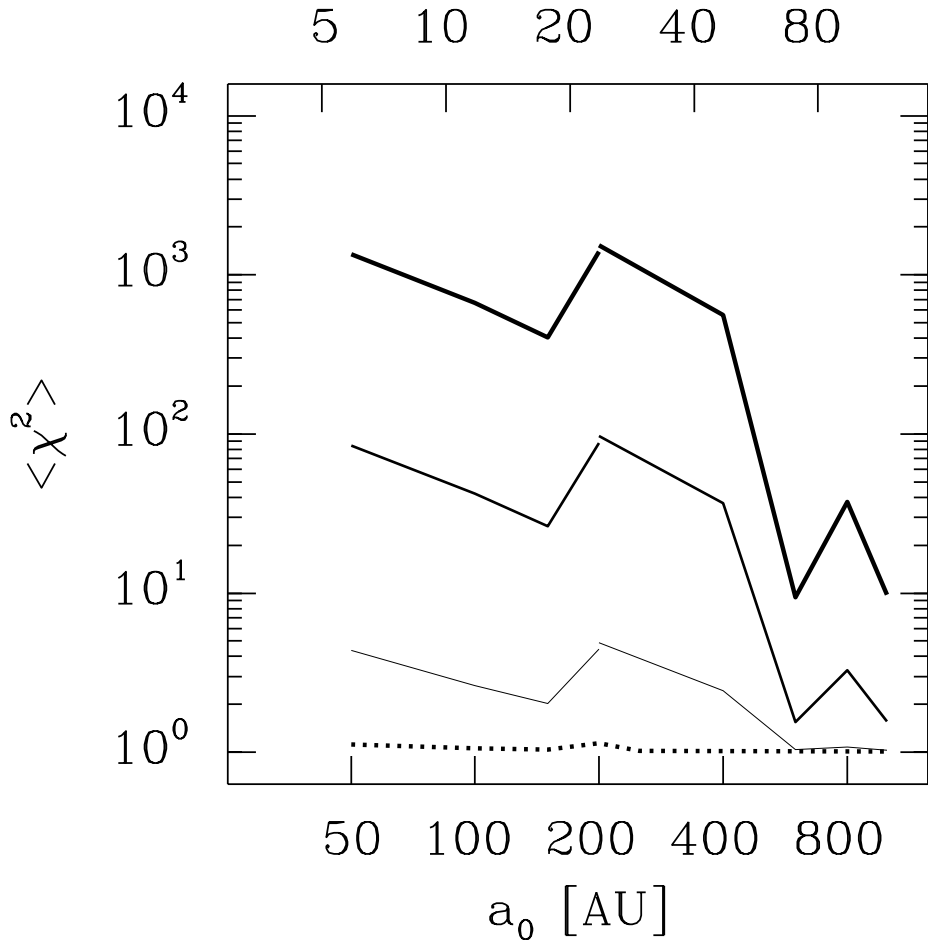


Figure 1: The averaged χ^2 per one degree of freedom for models neglecting periastron motion (solid lines) compared with the averaged χ^2 for models taking into account the periastron motion (dotted line). The fits were attempted for orbits of “true” semimajor axis $a_0 = 50$ to 1000 AU, which corresponds to periods $P_0 = 0.22$ to 19.6 y and angular sizes 6 to 118 mas. The results are shown for simulated observations with the astrometric accuracy of $\sigma = 0.17$ AU (20 μas , thick line), 0.68 AU (80 μas , medium line), and 3.4 AU (400 μas , thin line). Each model is based on 25 “observations” of star position which are not more frequent than five per period and not less frequent than once a year. That implies the dependence of the “observation strategy” on the orbit size.

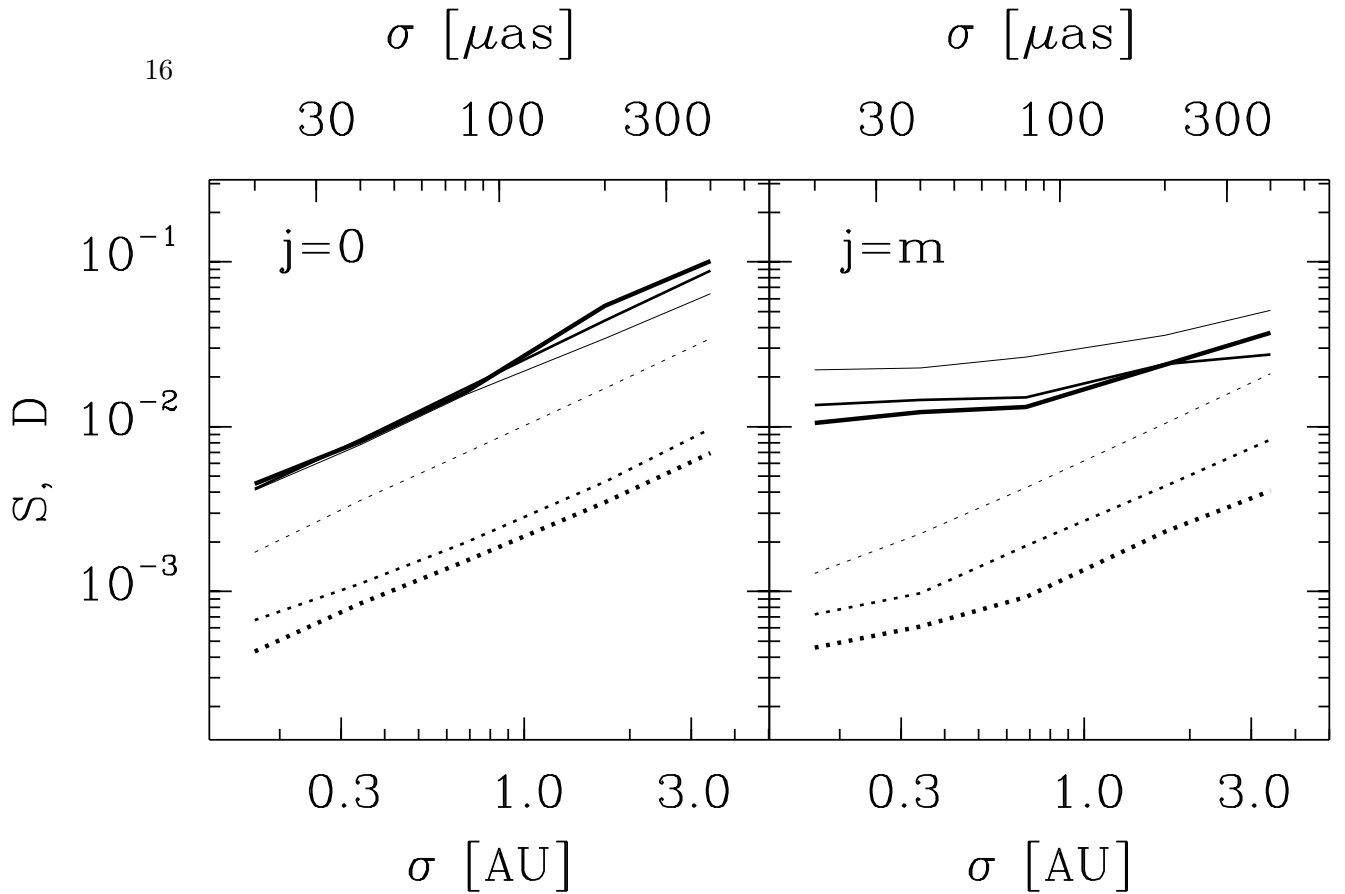


Figure 2: The relative difference between the fitted rate of the periastron motion and the rate expected for a nonrotating black hole of the same mass (solid lines) as a function of the accuracy of astrometric measurements. Also shown is the dispersion of the latter quantity (dotted lines). On the left panel the case of a nonrotating black hole is shown, and on the right panel - the hole rotating with the maximum angular velocity. The result are shown for the orbits of the semimajor axis $a = 50$ AU (thin), 150 AU (medium), and 250 AU (thick lines).

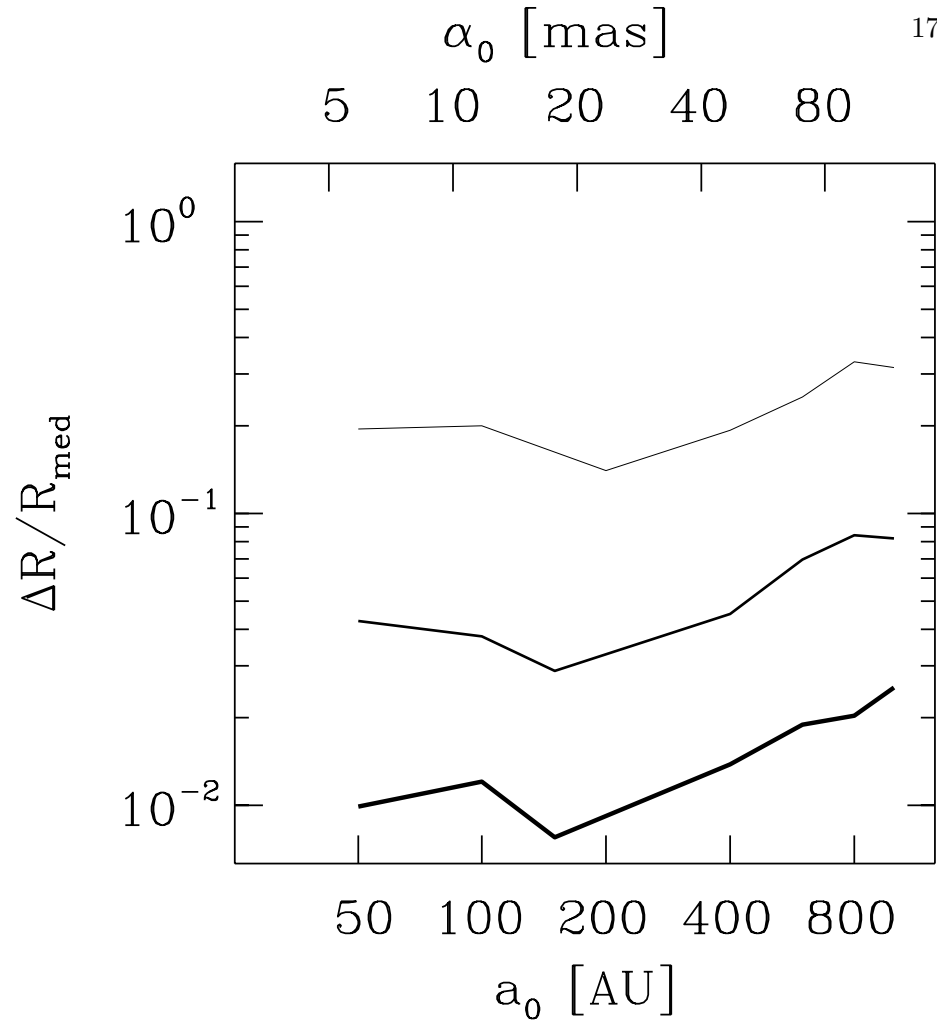


Figure 3: The typical error in the distance determination based on the measurement of periastron motion as a function of the orbit size. The results are shown for the astrometric accuracy of $20 \mu\text{as}$ (0.17 AU, thick line), $80 \mu\text{as}$ (0.68 AU, medium), and 0.4 mas (3.4 AU, thin).